Developing a Wireless Charging Concept Via Loosely Coupled Inductive Power Transfer for Mobile Applications

S. Saat, C. C. Heng, A. A. M. Isa, A. M. Darsono and M. S. M. Isa
Faculty of Electronic and Computer Engineering (FKEKK)
Universiti Teknikal Malaysia Melaka (UTeM), Malaysia
shakir@utem.edu.my

***Abstract*— This paper aims to develop a charging method for mobile applications, i.e electric vehicle via loosely coupled inductive power transfer (LCIPT) method. This method enables wireless power transmission from a stationary power source to a moving load, which is the electric vehicle in our case. In this paper, a prototype capable to deliver power efficiently from a stationary power source to a moving load is developed. The prototype is designed in a small scale low power model of 12 Volt 5 Watt DC input in order to prove the proposed method is applicable and could be widely used in future works through the evolution of wireless power transfer (WPT) technology. To be specific, in this project, Class E resonant inverter is used to convert the DC source to AC source at 1 MHz resonant frequency. Analysis is done on different configurations and setups of the transmission coils. Compensator circuit is also designed at the transmission coil to boost the power transfer efficiency. The output of the wireless power transmission is tested on DC-motorcar and LED. At the end, a prototype is successfully developed.**

***Index Terms*— Inductive power transfer, develop, WPT, stationary source, moving load, small scale model, low power prototype, LCIPT, electric vehicle**

I. Introduction

Fossil fuels and natural gases consumption have been increasing tremendously over the centuries since the invention of internal combustion engine (ICE) for automobile dated back to 1886, the first petrol or gasoline powered Benz Patent-Motorwagen, an invention of Karl Benz. The combustion of petrol and gasoline releases harmful gases to the atmosphere and pollutes the environment. Despite the effort to reduce the pollution with instalment of filters and engine-fuel combustion efficiency enhancement via the advent of technologies over the era, the fact that pollutants are still being emitted to the atmosphere remains. On top of that, fossil fuels and natural gases are non-renewable resources, and they are estimated to be depleted at the end of the 21st century [1]. Hence, alternative renewable energy resources such as electrical energy are being utilized to curb the problems in the automobile industry.

Electric vehicle (EV) is the alternative solution to reduce fuel consumption and pollution rate. The invention of electric vehicle is attributed to various people. A Hungarian inventor, Ányos István Jedlik invented the early type of electric motor in the year 1828 and created a small model car powered by that motor later. A Vermont blacksmith, Thomas Davenport built a similar small model electric car powered by electrified circular track [2].

One of the major advantages of the EV is that the need for eliminating fossil fuels or natural gases in modern transportation. The electric motor of the EV does not emit harmful gases to the atmosphere. Hence, the air pollution index could be reduced enhancing the air quality making EV environmentally sustainable. However, EV has several disadvantages that distaste the consumers' choice. The existing EVs have limited range up to 100 miles on road. A longer range would require a bigger cells storage which would consume the space in the vehicle. On top of that, due to the big cells storage, EV requires long recharging time, usually hours. Furthermore, the EVs are more expensive than the conventional medium-sized petrol-powered cars [3-6].

However, the availability of charging stations for EV is low and it takes a long time to completely charge an EV. This problem could be eliminated with wireless power charging technology via the loosely coupled inductive power transfer (LCIPT) method. Through the adoption of wireless power transfer (WPT) technology, the EV could be charged even at motion, providing flexibility, convenience and freedom from being bounded by plug-in power cords at charging point. At the present stage of the WPT technological level, LCIPT is still in the development stage and not ready for high power applications yet [7-15]. Some works that utilized Class E inverter can be found in [16-19], but none of them focusing on the electrical vehicle charging. Thus, this project focuses to develop the concept of LCIPT in a small scale low power model to prove the applicability of LCIPT in EV charging. With further improvements, the concept of motional EV charging could be realized.

The contribution of this paper can be summarized as follows:

1. The Class-E resonant inverter has been designed at 1Mhz frequency.
2. The suitable compensation circuit has been proposed to improve the performance of our IPT system.
3. Several coil setups have been done to see the best coil structure for the system

II. Research Design

The prototype is designed in a small scale low power model to represent the concept of electric vehicle (EV) charging via the loosely coupled inductive power transfer (LCIPT) method that adopts the approach of the wireless power transfer (WPT) technology. The operation process flow of the prototype model is illustrated in Figure 1.

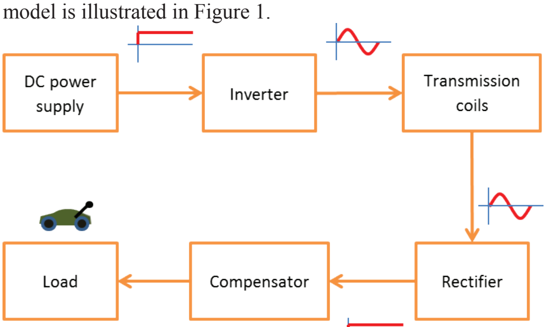

Figure 1: Prototype Model Operation Process Flow Block Diagram

The prototype model is powered by DC power supply as DC power supply is stable and consistent. As part of inductive power transfer (IPT), the transmission requires coupled magnetic resonance at certain resonant frequency between the transmitter and the receiver to transmit power. Hence, the DC power is then converted to AC power at the inverter before the transmission stage to provide magnetic resonance at a frequency of 1 MHz and to improve the transmission efficiency. At the transmission line, the primary coils at the transmitter induced the magnetic flux onto the secondary coil. The power output at the receiver-end of the transmission line is affected by the coils design; number of turn, shape of coil windings and type of coils. At the receiver, a rectifier is designed to rectify the induced AC power to DC for more stable and consistent output for the load. The rectifier is followed by a compensator circuit and voltage regulator to regulate the power losses in the transmission line. In this case, the load used the RC-car to represent the EV.

A. *Class E Resonant Inverter Circuit*

The Class-E inverter is designed and simulated with LTspice software. Through LTspice software, the zero voltage switching can be confirmed at the class-e MOSFET switch. This design is referred to [18-21].

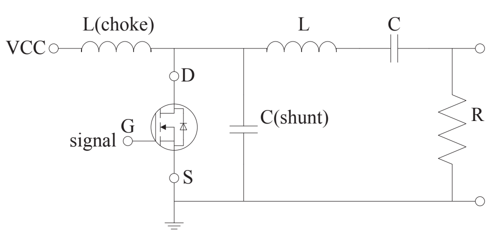

Figure 2: Class E Resonant Inverter Circuit

The inverter design as shown in Figure 2 consists of a single N-MOSFET switch and a resonant tank. The switching signal in which Pulse Width Modulation (PWM) signal is supplied by the Peripheral Interface Controller (PIC) as PIC is capable of supplying a stable and consistent signal at high frequency.

For Class E inverter, the choke inductance has no specific calculation for the best value. However, the minimal value must be met and it is best to select higher value of 100 µH or 1 mH. The minimal value of choke inductance can be determined by the following formula:

$$L_{choke} = \frac{0.4001R}{2\pi f} \quad (1)$$

Meanwhile, the resonant tank parameter can be calculated using the following formulae as described in [18].

The operating current, I_o is calculated as follows:

$$I_o = \frac{P_{Load}}{V_{CC}} \quad (2)$$

Meanwhile, the shunt capacitance is calculated using the following formula:

$$C_{shunt} = \frac{I_o}{2\pi^2 f V_{CC}} \quad (3)$$

Then, the resonant tank load resistance is calculated as:

$$R_{Load} = \frac{8{V_{CC}}^2}{(\pi^2+4)P_{Load}} \quad (4)$$

On the other hand, the resonant tank series inductance is calculated as:

$$L = \frac{QR}{2\pi f} + \frac{1.153R}{2\pi f} = \frac{R(Q+1.153)}{2\pi f} \quad (5)$$

Finally, the resonant tank series capacitance is calculated using the following formula:

$$C = \frac{I_o}{2\pi f Q R} \quad (6)$$

B. *Wireless Power Transmission Coil Design Method*

In this project, two different approaches of transmission coil design for Class E inverter are considered. The first method (Design Method 1) is to tap power output from the load, R, of the Class E inverter with a serial compensator (capacitor). This serial compensator will increase the power output at the load of the Class E inverter. The second design method is to alter the Class E inverter itself into wireless power transmission device. This can be done by replacing the resonant tank inductor, L, of the Class E inverter into transmission coil and the resonant tank load into the DC-motorcar.

The above two methods of transmission coil are illustrated in the following figures:

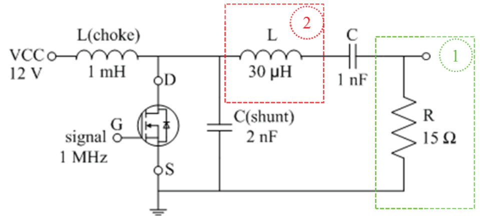

Figure 3: Transmission Coil Design Methods on Class E Inverter

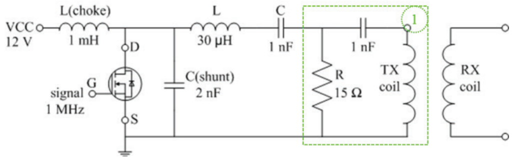

Figure 4: Transmission Coil Design Method 1 [28]

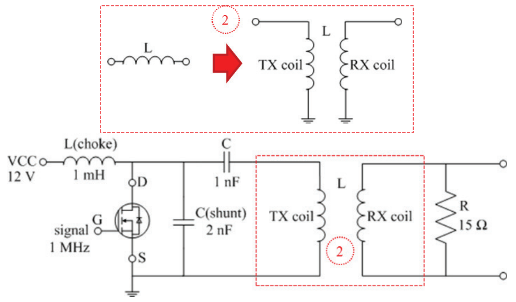

Figure 5: Transmission Coil Design Method 2 [32]

In this project, Design Method 1 is more suitable, and is more stable in power transmission. The resonant tank of the Class E inverter circuit is not disturbed or altered. This retains the resonance and the zero voltage switching throughout the power transmission. Due to the loosely coupled inductive power transfer approach used in this project and the fact that the transmission coils are irregular as they are hand-turned, the moving receiver (RX coil) will cause the inductance to fluctuate, hence disturbing the resonance of the Class E inverter resulting in the failure to achieve zero voltage switching. Based on this consideration, Design Method 1 is chosen for this project.

The final circuit parameters are tabulated in Table 1.

Table 1
Circuit Parameters of Class E Resonant Power Converter Circuit

Circuit Parameters	**Values**
Power MOSFET, NMOS	IRF510
Operating Frequency, f_o	1MHz
Input DC supply, V_{dc}	12.0V
Rated Power, P_o	5.0W
Operating Current, I_o	0.42A
Choke Inductor, L_{choke}	1.0mH
Shunt Capacitor, C_{shunt}	1.8nF
Series Capacitor, C_{series}	1.0nF
Series Inductance, L_{series}	30.0µH
Primary Serial Capacitor Compensation, C_1 and C_2	1.0nF
Load Resistance, R_L	16Ω

III. Main Results

A. Class E Resonant Inverter Zero Voltage Switching

The measurements taken are Gate voltage V_G, Drain voltage V_D, resonant tank series capacitor voltage V_C, and load voltage V_R. The labels of respective measurements are as shown in Figure 6 and Figure 7.

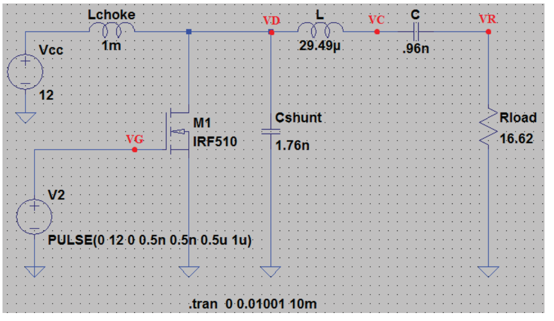

Figure 6: Class E Inverter Circuit using LTspice

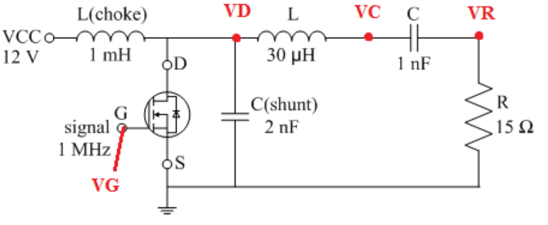

Figure 7: Practical Class E Inverter Circuit

For practical implementation, the component values are chosen to the closest value available. Hence, the results obtained from the simulation and practical may differ slightly.

The design of the Class E Inverter is simulated with LT-Spice software. The Drain-Gate voltage graph is simulated to determine the zero voltage switching (ZVS) and compared with the practical oscilloscope result.

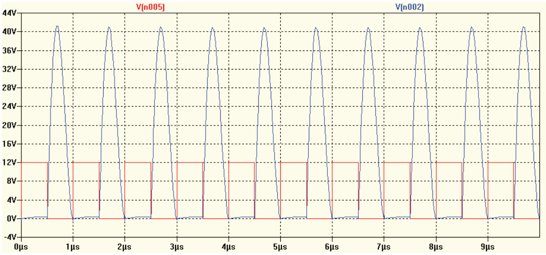

Figure 8: Drain V_D (Blue) vs. Gate V_G (Red) ZVS [Simulation]

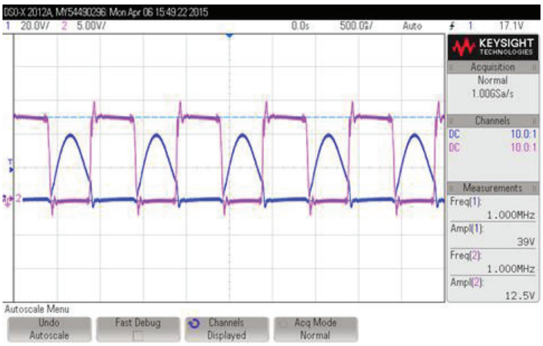

Figure 9: Drain V_D (Blue) vs. Gate V_G (Purple) ZVS [Practical]

The ZVS is achieved in both practical as shown in Figure 8 and Figure 9. With ZVS achieved, the power loss on the transmitter side could be reduced, thus improving the transmission efficiency.

The resonant tank capacitor voltage V_C and the load voltage V_R are also simulated as shown in Figure 10 and compared with the practical one, as shown in Figure 11.

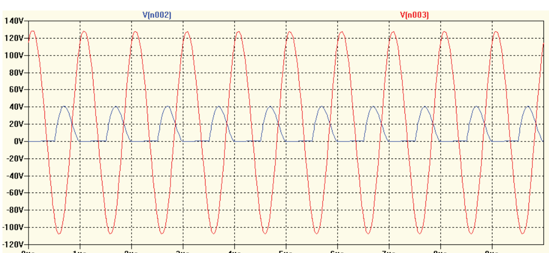

Figure 10: Drain V_D (Blue) vs. Capacitor V_C (Red) [Simulation]

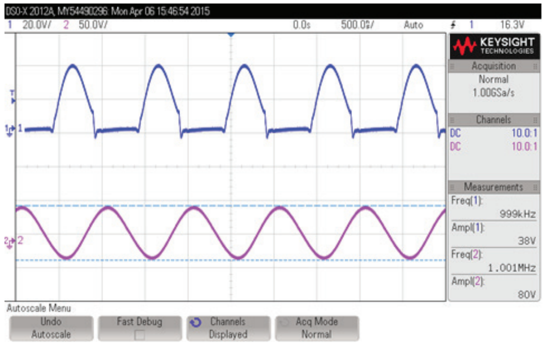

Figure 11: Drain V_D (Blue) vs. Capacitor V_C (Purple) [Practical]

The resonant tank series capacitor voltage V_C shows a great voltage output and a tendency for power transmission. However, when the transmitter TX-coil is connected to the V_C point and ground, the transmitter circuit (Class E inverter) is overloaded and the DC power supply limits the power input to the circuit. Increasing the current limit on the DC power supply resulted in overloading and burning of the components.

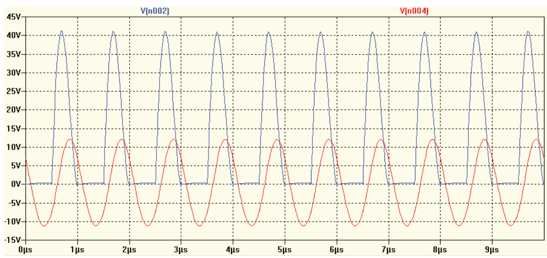

Figure 12: Drain V_D (Blue) vs. Load Resistor V_R (Red) [Simulation]

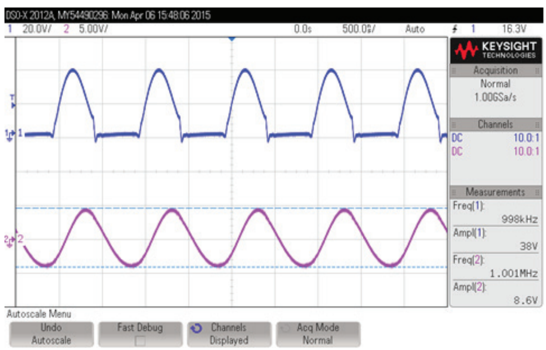

Figure 13: Drain V_D (Blue) vs. Load Resistor V_R (Purple [Practical]

Meanwhile, the load voltage V_R output is lower in the practical than the simulation as in Figure 12 and 13 respectively. However, the power output is much more stable than the V_C point. When the TX-coil is connected parallel to the load resistor, the voltage did not change and the power output remained the same as the output from the Class E load resistor. The results are tabulated in Table 2.

Table 2
Class E Resonant Inverter Voltage Output

Approach	V_G (V)	V_D (V)	ZVS	V_C (V)	V_R (R)
Simulation	12.0	40.0	Achieved	130.0	12.0
Practical	12.5	38.0	Achieved	80.0	8.6

B. Transmission TX-RX Coil Results and Analysis

The circuit setup for the following experiments is as shown in Figure 4.

Experiment 1 – Circular TX-Coil

For this test analysis, the copper coil is used as the transmitter coil and the litz wire coil is used as the receiver coil. The litz wire coil has fixed (N_{RX}) 20 turns with ferrite core. The copper coil is 0.25 mm in diameter. The thickness of the board (d_{TRACK}) used for the track is 3 mm. The transmitter core (d_{CORE}) is 1.3 cm in length and the coil is turned from the bottom of the core by hand. The output voltages measured are AC output from the TX-coil and RX-coil. Figure 14 shows the circular TX-coil track installation with following parameters:

Fixed parameters:

- Copper coil 0.25 mm diameter;
- d_{TRACK} = 3 mm;
- d_{CORE} = 1.3 cm;
- N_{RX} = 20 turns

Variable parameters:

- Number of turns in transmitter coil (N_{TX})
- TX-RX coil alignment; edge to centre
- Gap from coil to core track surface (d_{GAP})

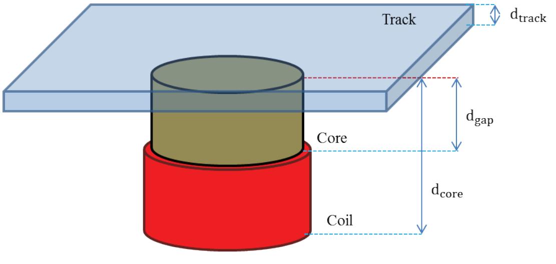

Figure 14: TX-Coil Track Installation

The results are recorded in Table 3.

Table 3
Transmission Coil Efficiency Test Analysis

N_{TX}	L_{TX} (mH)	V_{TX} (V)	V_{RX} (V) Edge-Centre	d_{GAP} (cm)	Coil Ratio, R	$V_{RX(max)}$ (V)	Efficiency (%)
10	0.02029	8.2	1.09 – 3.76	0.8	2	16.4	22.93
20	0.06018	8.4	1.05 – 2.65	0.5	1	8.4	31.54
30	0.11014	11.1	1.05 – 2.53	0.4	0.67	7.4	34.19
50	0.30011	8.2	0.70 – 1.25	0.2	0.4	3.28	38.12
100	0.90220	10.7	0.40 – 0.96	0.1	0.2	2.14	44.86

The inductance of the TX-coil is measured using the Digital L.C.R. Meter EDC-1630. The calculations are:

$$\text{Coil Ratio, R} = \frac{N_{RX}}{N_{TX}} \tag{7}$$

$$V_{RX(max)} = R \times V_{TX} \tag{8}$$

$$\text{Efficiency} = \frac{V_{RX(centre)}}{V_{RX(max)}} \times 100\% \tag{9}$$

Experiment 2- Elongated TX-Coil

The TX-coil is now designed in an elongated manner, while the RX-coils used are litz wire coil and the hand-turned 0.25 mm copper coil for comparison. The TX-coil build is as shown in Figure 14 and Figure 15 and it is hand-turned. Coil length is a = 10 cm.

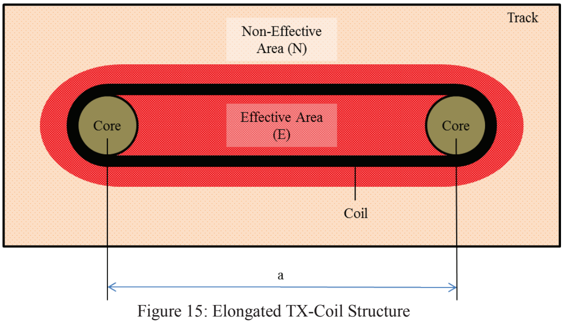

Figure 15: Elongated TX-Coil Structure

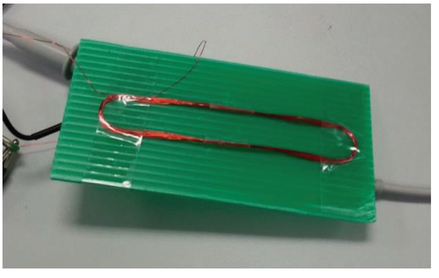

Figure 16: Elongated TX-Coil

The DC power supply settings are set to 12 V and current limit to 0.22 A. When the coil is installed on the Class E inverter load resistor, the TX-coil voltage is measured at V_{TXO} = 8.6 V. The same 3mm thick board as in Experiment 1 is used as a track. The TX-coil is now taped to the board as shown in Figure 16 rather than coiled on the ferrite core as in Figure 14. The ferrite core is then placed under the coil for core-presence analysis. The transmission voltage is measured from end-to-end about the effective and non-effective area. The output voltages measured are AC output from the TX-coil and RX-coil. The result is tabulated in Table 4.

Table 4
Elongated TX-Coil Transmission Analysis (Current Overloaded)

Type	N_{TX}	N_{RX}	Core Presence	V_{TX} (V)	$V_{RX(N)}$ (V)	$V_{RX(E)}$ (V)
Litz wire	10	20	×	12.0	0.6 – 1.3	3.0 – 4.8
			✓	20.1	0.9 – 2.5	4.2 – 9.8
Copper	10	20	×	10.1	0.38 – 0.96	3.24 – 4.02
			✓	24.9	2.8 – 4.4	6.0 – 18.5
Copper	10	30	×	13.1	1.4 – 2.6	5.6 – 9.8
			✓	24.9	2.8 – 5.2	7.2 – 34.6
Litz wire	20	20	×	21.7	0.28 – 1.13	2.53 – 4.14
			✓	19.3	0.6 – 1.3	3.1 – 5.1
Copper	20	20	×	22.5	0.6 – 1.4	3.9 – 4.7
			✓	18.9	0.6 – 2.0	3.3 – 7.2

*$V_{RX(N)}$ is the voltage measured along the non-effective area and
*$V_{RX(E)}$ is the voltage measured along the effective area

As current is limited to 0.22A from the power supply, the circuit is overloaded, causing the DC power supply turned into a Constant Current (CC) mode. Thus, the voltage output measured is higher than the expected value. This result is not accurate and not suitable for the applications of the battery powered source as the battery source does not provide constant current throughout its supply span. The mutual inductance between the transmission TX-RX coils increases the transmitter voltage, V_{TX} .

The DC power supply current limit is adjusted slightly higher to 0.3 A to eliminate the current overloading issue. Higher current limit setting will burn the components in the Class E inverter as the power rating of the lump components are not high enough. The result is tabulated in Table 5.

Table 5
Elongated TX-Coil Transmission Analysis (Current Not Overloaded)

Type	N_{TX}	N_{RX}	Core Presence	V_{TX} (V)	$V_{RX(N)}$ (V)	$V_{RX(E)}$ (V)
Litz wire	20	20	×	14.7	0.28 – 0.88	2.21 – 3.06
			✓	13.5	0.28 – 1.45	1.77 – 3.70
Copper	20	20	×	15.5	0.36 – 0.56	1.89 – 2.61
			✓	13.1	0.36 – 0.60	1.87 – 3.90
Copper	20	40	×	15.4	0.60 – 1.13	2.17 – 3.10
			✓	14.7	0.42 – 1.61	1.53 – 4.06

*$V_{RX(N)}$ is the voltage measured along the non-effective area and
*$V_{RX(E)}$ is the voltage measured along the effective area

When the current limit is increased, the Class E inverter is no longer overloaded. The transmission output voltage results are much lower because the DC power supply is not in the CC mode. As the number of coil turns is low, the efficiency is low, and thus the voltage output is low even when the mutual inductance increased the transmitter voltage, V_{TX}.

However, when the coil is reconstructed to about the length, a = 50 cm in the presence of core, N_{TX} = 20 and N_{RX} = 40, the performance of the power transfer dropped significantly. The voltage output as shown in Figure 17 is only 1.35 V at the effective area.

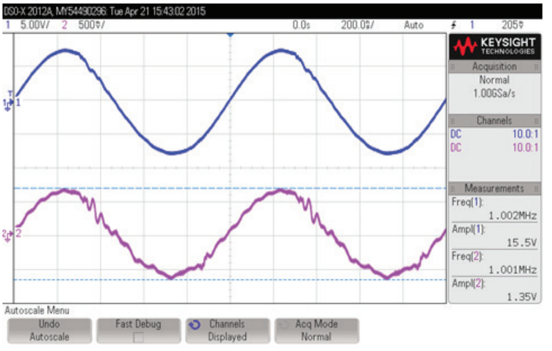

Figure 17: Elongated TX-Coil (a=50cm); V_{TX} (Blue vs. V_{RX} (Purple)

The V_{TX} does not differ much from the coil length, a = 10 cm build as the mutual inductance remained the same. However, as the coil length increases, the losses increase lowering the output voltage.

Experiment 3 – Parallel Circular TX-Coil

In contrast to Experiment 2, the TX-coil in this experiment is constructed in a parallel circular manner. Each circular coil has N_{TX} = 20 turns. The RX-coil used in this experiment has N_{RX} of about 120 turns. The TX-coil design is further illustrated in Figure 18 and Figure 19.

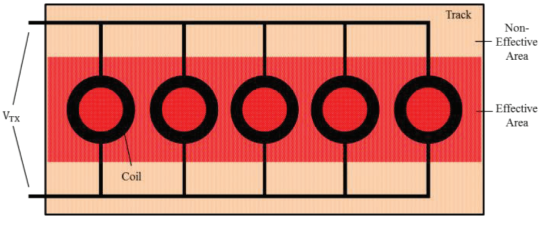

Figure 18: Parallel Circular TX-Coil Structure

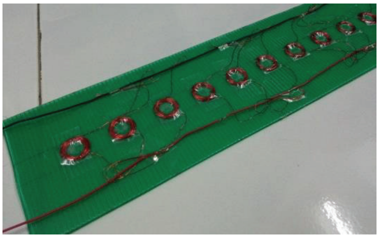

Figure 19: Parallel Circular TX-Coil

When the parallel circular TX-coil is connected to the load resistor of the Class E inverter, the coil input V_{TX} dropped significantly. This is because each circular coil has resistance and the equivalent resistance is lowered when the coils are connected in parallel to the Class E inverter load resistor. Thus, the voltage dropped as the load resistance is lowered as shown by Amp(1) in Figure 20 and Figure 21.

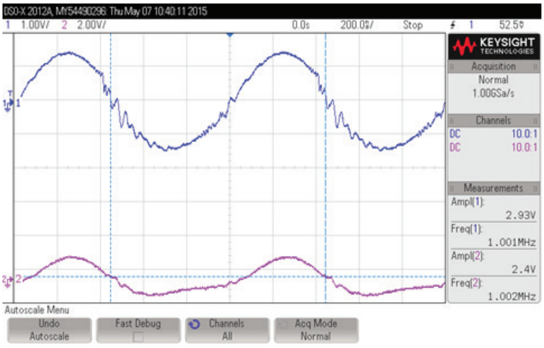

Figure 20: Parallel Circular TX-Coil without Core; V_{TX} (Blue) vs. V_{RX} (purple)

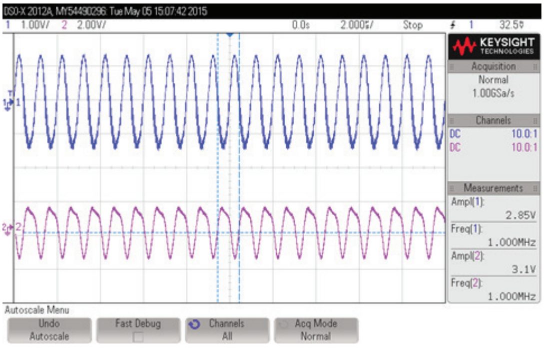

Figure 21: Parallel Circular TX-Coil with Core; V_{TX} (Blue) vs. V_{RX} (purple)

The drop-in the transmitter voltage, V_{TX} results in low output voltage, V_{RX}. As the ratio of the TX-RX coil is 1:6, this result shows that the power transmission is not efficient with this coil configuration. Furthermore, when the RX-coil move along the TX-coil track, the output voltage simultaneously turned on and off as the magnetic flux is not cut between each circular TX-coil.

C. DC-motor Power Requirement Analysis

The DC-motorcar requires two AA –batteries (2 x 1.5 V) to operate. The DC-motorcar used in the project is about 10 cm wide by 15 cm length. The DC-motorcar used is shown in Figure 22.

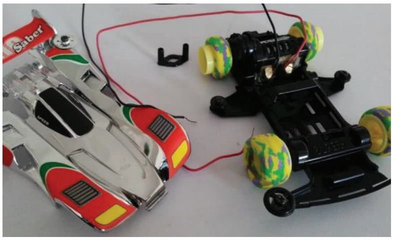

Figure 22: DC-Motorcar used for Project Prototype

The DC-motorcar input power is directly connected the DC power supply. The current limit is adjusted to a minimum of 0.1 A. The input voltage is set to 0 V. The DC-motorcar is first tested with voltage input setting tuned from 0 V to 30 V. Current limit overloaded and the DC power supply turned into CC mode. High power with limited current does not run the DC-motor.

The current limiter is then adjusted, while the input voltage is set to 0.1 V. The current limit is slowly increased from 0.1 A to 2.0 A. The DC-motor does not run. A high current but insufficient voltage will not drive the DC-motor.

Both current limit and input voltage are then set to a minimum 0.1 A and 0 V. Both probes are then adjusted to analyse the DC-motor power requirement. The results are tabulated in Table 6.

Table 6
DC Power Supply Settings on DC-Motorcar Analysis

Current Limit (A)	Input Voltage (V)	Description
0.1	0.0	Initial minimum settings.
0.5	0.5	DC-motor did not run.
1.0	0.5	DC-motor did not run.
1.5	0.5	DC-motor did not run.
2.0	0.5	DC-motor did not run.
0.5	1.0	DC-motor did not run. The motor ran with a little push but very slowly and then stop after few seconds.
1.0	1.0	DC-motor did not run. The motor ran constantly with a little push at moderate speed.
1.5	1.0	DC-motor ran constantly at high speed
2.0	1.0	DC-motor ran constantly at maximum speed.
1.0	2.0	DC-motor ran constantly at moderate speed.
1.5	2.0	DC-motor ran constantly at maximum speed.

The results show that the DC-motor requires at least a minimum current and a voltage 1.0 A and 1.0 V to operate. Since the operating current, I_O, of the prototype is only 0.4 A as calculated in Section II, the minimum current requirement is not met even though the voltage transferred is more than required. Thus, the load is replaced by LED in order to prove that the LCIPT is able to transfer power wirelessly to a moving load as analyzed in the following section.

D. LED Moving Load Analysis

The LED is tested on the receiver side by placing the LED directly to the RX-coil (AC power) and through rectifier (DC power). The TX-coil used in this experiment are the parallel circular TX-coil as designed in Figure 19 and a newly fabricated PCB coil as shown in Figure 23 to replace the inefficient elongated TX-coil as designed in Figure 16. The ferrite core is placed on the RX-coil to improve the received power signal waveform.

Figure 23: Elongated PCB TX-Coil

As the PCB TX-coil is installed onto the inverter, the input transmission voltage, V_{TXO}, dropped from 8.6 V to 6.4 V due to the parallel resistances between the coil and the load of the inverter. The LED lights up as the RX-coil moves along the effective area of the track with and without rectifier.

Meanwhile, as the parallel circular TX-coil is installed onto the inverter, the input transmission voltage, V_{TXO}, dropped significantly from 8.6V to 3.4 V. This is due to the resistance of the parallel alignment of each circular coils and the load of the inverter greatly reduced the resistance and thus causing the voltage drop. The LED lights up when it is placed directly aligned on the circular coil. The LED blinked as the RX-coil moves along the track. This shows that the magnetic flux in the transition zone between the circular coils does not cut with the direction of RX-coil motion.

E. Overall Discussions

As the prototype designed has insufficient current to power up the DC-motor, the load is replaced with and LED. The LED is tested moving with and without rectifier along the track on both field effective and non-effective area on both elongated and parallel circular TX-coil designs. The LED lights up even on the raw AC output of the RX-coil. This shows that the advantage of high frequency AC power is capable of supplying almost constant DC power to the load from both positive (+V) and negative (-V) cycles. This shows that the concept of wireless power transfer via loosely coupled inductive power transfer method is possible and achievable with further researches and developments.

There are many obstacles faced upon completing this small scale low power prototype. First of all, the design of 5 W, 12 V small scale low power prototype has operating current of I_O of 0.4 A. As analyzed in Section III, the DC-motorcar requires at least minimum current of 1.0 A and voltage of 1.0 V to operates. During the experiments, the supplied current is limited to 0.4 A, which is the operating current of the designed Class E inverter circuit. Tuning the current limit higher than 0.4 A will burn up the circuit components when the circuit is overloaded. This setting itself did not provide sufficient current to drive the DC-motor at the other end, not considering the losses yet. The idea to boost the current with DC-DC boost converter is not applicable because the converter needs a constant V_{CC} to operate. As for this loosely coupled approach used in this project, the output power fluctuates as the RX-coil move along the TX-coil track.

The circuit often overloads when the transmission coils are connected due to the power transmission drawing high current for transmission. Increasing the supply current limit will overcome this issue, but it will burn the components in the Class E inverter. This is because the components used are common lump components with low power rating. High power rating components are expensive and not affordable in this low budget project. The circuitry works best if the circuit is built with surface mount high power rating components used in industries. However, this idea could not be realized due to the budget limitation. The component that often burns up is the capacitor and the inductor. To overcome this issue, the capacitors are connected in parallel to increase the power rating. Instead of using one capacitor of the nearest value, the parallel connection sums up the value to the nearest capacitance value needed for the circuitry. For the inductor, the inductor is custom coiled with a ring ferrite core and copper wire. The inductance is then measured with Digital L.C.R. Meter EDC-1630 available in the laboratory and further modified to reach the nearest inductance value needed.

The power transmission efficiency of the TX-RX transmission coil in the prototype built is very low. This is due to the coils are being hand-turned and they are irregular in shape. This affects the flux distribution throughout the effective area. Distortions and neighbouring flux interferences reduced the power transmission efficiency significantly. As the power is transmitter wireless via induction, the transmission medium plays a crucial role in the power transmission efficiency. Magnetisation capability of the medium material affects the flux density, B, and air has the lowest flux density saturation compared to iron and steel according to the Magnetisation (B-H) Curve as in Figure 24.

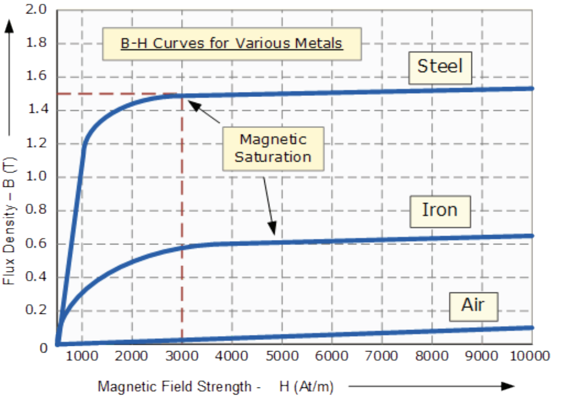

Figure 24: Magnetisation (B-H) Curve [22]

The approach of loosely coupled inductive power transfer (LCIPT) used in this project is to eliminate the need of transmission medium as in transformer and enables the freedom of motion during power transmission but at the cost of efficiency drop.

The power transmission efficiency of this approach is improved by better design of TX-coil instalment on track. The TX-coil is taped under the corrugated plastic board (track) to remove the core gap and thus reduce the transmission gap to only the thickness of the plastic board, which is 3 mm. This design produced better results than the previous design, which is the coil is turned around the cylinder core. The design is illustrated in Figure 25.

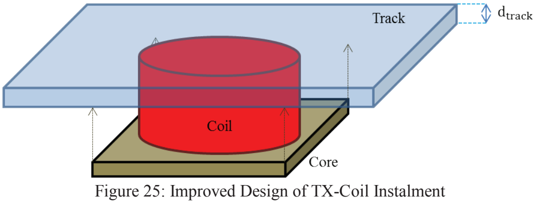

Figure 25: Improved Design of TX-Coil Instalment

The best core to be used on this design is flat-plated ferrite core. However, this type of core is hard to be found on store as commercial ferrite cores are produced in cylindrical shaped.

IV. CONCLUSION

The concept of moving load wireless charging, which enables the freedom of motion during charging is proven possible and achievable. However, the efficiency of this loosely coupled method approach is much lower than the properly coupled magnetic resonance method. In exchange for freedom of motion while charging, this concept pays the cost with its efficiency. Nevertheless, the power transmission efficiency in this research is low because the prototype model is mostly hand-crafted, including the coils windings. However, the efficiency can be increased with high power input and better transmission coils design. The low power input design of this project limits the current supply, thus reducing the magnetisation field strength in the transmission coils. Hence, the lower induction power resulted in low efficiency power transfer. Due to the many limitations such as resource funds and component choices, the current rating could not be improved and thus the prototype has low power transmission efficiency and is not capable to drive the 1.5 A DC-motorcar. A LED is used to show that the power transfer is possible as the load moves across the field effective area on the track and the concept is proven possible and achievable. Notice that in this work, the designed Class E inverter load is mismatched with the real load; therefore the efficiency obtained in this paper is not good enough. Therefore, it is best to see in the future the performance of the system if the mentioned resistance value is matched to each other.

.

REFERENCES

[1] Nelder, C. (2009, July 24), *"The End of Fossil Fuel"*, [Online] Forbes, Available: http://www.forbes.com/2009/07/24/peak-oil-production-business-energy-nelder.html

[2] "*Today in Technology History: July 6"*, The Center for the Study of Technology and Science, July 14, 2009.

[3] Berman, B. (2014, October 14), "*Electric Cars Pros & Cons"*, [Online] Plugincars, Available: http://www.plugincars.com/electric-cars-pros-and-cons-128637.html

[4] Y. Chen, "Integration of Electric Vehicle Charging System into Distribution Network", *Power Electronics and ECCE Asia (ICPE & ECCE), 2011 IEEE 8th International Conference on*, On page(s): 593 – 598

[5] I.S. Suh, "Electri Vehicle On-Road Dynamic Charging System with Wireless Power Transfer Technology", *Electric Machines & Drives Conference (IEMDC), 2013 IEEE International*, On page(s): 234 – 240

[6] F. Locment, "Electric Vehicle Charging System with PV Grid-Connected Configuration", *Vehicle Power and Propulsion Conference (VPPC), 2010 IEEE*, On page(s): 1 – 6

[7] L.K. Gao, "Design of Energy Feedback Mode Wireless Charging System for Electric Vehicles", *Industrial Electronics and Applications (ICIEA), 2013 8th IEEE Conference on*, On page(s): 1827 – 1831

[8] S. Mohaghehi, "Inductive Power Transfer for Electric Vehicles: Potential Benefits for Distribution Grid", *Electric Vehicle Conference (IEVC), 2012 IEEE International*, On page(s): 1 – 8

[9] R. Biswa, "Feassibility of Wireless Power Transmission", Electronics & Communication Engineering, College of Science & Technology Rinchending, Phuentsholing, India, May 2012

[10] X.Z. Wei, Z.S. Wang, H. F. Dai, "A Critical Review of Wireless Power Transfer via Strongly Coupled Magnetic Resonance", Energies 7, no. 7:, pp. 4316-4341, 2014

[11] A. Kurs, A. Karalis, R. Moffatt, J. D. Joannopoulos, P. Fisher, M. Soljacic, "Wireless Power Transfer via Strongly Coupled Magnetic Resonances", in Science Express on 7 June 2007, Vol. 317. no. 5834, pp. 83 – 86

[12] T. lmura, Y. Hori, "Wireless power transfer using electromagnetic resonant coupling", The Journal of the Institute of Electrical Engineers of Japan, Vol. 129, No. 7, pp.414-417, 2009

[13] O.H. Stielau, "Design of Loosely Coupled Inductive Power Transfer Systems", *Power System Technology, 2000 Proceedings, PowerCon 2000, International Conference on ,Volume 1*, On page(s): 85 – 90

[14] N. Jamal, "A Study on Performances of Different Compensation Topologies for Loosely Coupled Inductive Power Transfer System", *Control System, Computing and Engineering (ICCSCE), 2013 IEEE International Conference on*, On page(s): 173 – 178

[15] Z.X. Mao, "Characteristic & Design of Transformer in Loosely Coupled Inductive Power Transfer System", *Electrical and Control Engineering (ICECE), 2010 International Conference on*, On page(s): 3454 – 3457.

[16] S. Aldhaher, "Wireless Power Transfer Using Class E Inverter With Suitable Saturable DC-Feed Inductor", *2014 Industry Applications, IEEE Transactions on, Volume 50, Issue 4*, On page(s): 2710 – 2718

[17] F.B. Chen, "Zero Voltage Switching Operation of a Push-Pull Resonant Converter with Slow Feedback Loop and Online Communication", *Industrial Technology (ICIT), 2013 IEEE International Conference on*, On page(s): 644 – 649

[18] J. Norezmi, S. Shakir, Y. Yusmarnita, Z. Thoriq, M.S.M. Isa and A.A.M. Isa, "Investigation on Capacitor Compensation Topologies Effects of Different Inductive Coupling Links Configurations", International Journal of Power Electronics and Drive System (IJPEDS), 2014

[19] N. Jamal, S. Saat, and Y. Yusmarnita, "A Development of Class E Converter Circuit for Loosely Coupled Inductive Power Transfer System," WSEAS Trans. CIRCUITS Syst., vol. 13, pp. 422–428, 2014.

[20] M.K. Kazimierczuk, D. Czarkowski, "Class E Zero Switching-Voltage-Switching Resonant Inverter", in Resonant Power Converters, 2nd edition, Wiley-IEEE Press, 2011, pp. 334 – 381

[21] W.L. Dai, W. Tang, Y.X. Xiao, J.T. Fei, "A Wireless Power Transfer System Based on Class E Amplifier", *Jiangsu Key Laboratory of Power Transmission and Distribution Equipment Technology, 2013 13th International Conference on Control, Automation and Systems (ICCAS 2013),* On page(s): 55 – 63

[22] "Magnetic Hysterisis", [Online], Electronics Tutorials, Available: http://www.electronics-tutorials.ws/electromagnetism/magnetic-hysteresis.html.